Supporting Information for World Wide Web Edition

Exploring the binding mechanism of UDP-galactopyranose to UDP-galactopyranose mutase by STD-NMR spectroscopy and molecular modeling†

Yue Yuan[‡§], *Xin Wen*[‡§], *David A. R.Sanders*[¶] *and B. Mario Pinto*[‡*]

[‡]Department of Chemistry, Simon Fraser University, Burnaby, British Columbia, Canada V5A 1S6

[¶]Department of Chemistry, University of Saskatchewan, 110 Science Place, Saskatoon, Saskatchewan, Canada S7N 5C9

[§]These authors contributed equally to this work.

[*]Addressed correspondence to B. Mario Pinto, Department of Chemistry, Simon Fraser University, Burnaby, British Columbia, Canada V5A 1S6. Tel: 604-291-4152; Fax: 604-291-4860; E-mail: bpinto@sfu.ca.

FUNDING This work was supported by Discovery Grants administered by the Natural Sciences and Engineering Research Council of Canada to both BMP and DARS.

RUNNING TITLE Ligand Binding to UDP-Gal*p* Mutase by STD-NMR/Modeling

Table 1. Calculated energies of UDP-Gal*p* **1,** UDP **2** and Gal*p* 1-phosphate **3** docked in the active site of UGM.

UDP-Gal*p* **1**			UDP **2**			Gal*p* 1-phosphate **3**		
Cluster rank[a]	Docked energy (kcal mol^{-1})	Mean docked energy (kcal mol^{-1})	Cluster rank[a]	Docked energy (kcal mol^{-1})	Mean docked energy (kcal mol^{-1})	Cluster rank[a]	Docked energy (kcal mol^{-1})	Mean docked energy (kcal mol^{-1})
1 (24)	-14.31	-12.30	1 (185)	-10.38	-9.57	1 (44)	-7.51	-7.08
2 (21)	-13.82	-11.45	2 (30)	-9.55	-8.98	2 (18)	-7.39	-7.04
3 (71)	-13.52	-11.62	3 (3)	-9.02	-8.85	3 (27)	-7.38	-7.08
4 (10)	-13.03	-11.69	4 (4)	-9.01	-8.88	4 (13)	-7.33	-6.94
5 (41)	-13.03	-11.66	5 (14)	-8.75	-8.50	5 (2)	-7.30	-7.09
6 (14)	-12.93	-10.82	6 (4)	-8.68	-8.42	6 (124)	-7.19	-6.88
7 (37)	-12.75	-11.08	7 (5)	-8.66	-8.41	7 (35)	-7.04	-6.71
8 (16)	-12.73	-11.54	8 (13)	-8.61	-8.32	8 (8)	-7.03	-6.88
9 (29)	-12.71	-10.50	9 (1)	-8.58	-8.58	9 (7)	-6.97	-6.77
10 (14)	-12.59	-11.57	10 (3)	-8.56	-8.04	10 (1)	-6.93	-6.93
11 (9)	-12.54	-10.57	11 (3)	-8.46	-8.39	11 (4)	-6.89	-6.77
12 (5)	-12.38	-10.46	12 (3)	-8.32	-7.95	12 (7)	-6.84	-6.74
13 (2)	-12.24	-9.63	13 (4)	-8.26	-8.05	13 (3)	-6.73	-6.64
14 (10)	-12.14	-10.51	14 (3)	-8.21	-8.01	14 (1)	-6.55	-6.55
15 (10)	-12.06	-10.12	15 (2)	-8.17	-7.82	15 (3)	-6.48	-6.32
16 (3)	-11.99	-10.73	16 (6)	-8.14	-7.99	16 (1)	-6.39	-6.39
17 (3)	-11.98	-9.58	17 (1)	-8.08	-8.08	17 (1)	-6.35	-6.35
18 (8)	-11.91	-10.49	18 (6)	-8.08	-7.85	18 (1)	-6.28	-6.28
19 (1)	-11.85	-11.85	19 (2)	-8.06	-7.89			
20 (2)	-11.79	-11.47	20 (1)	-7.99	-7.99			
21 (10)	-11.50	-9.90	21 (3)	-7.88	-7.73			
22 (1)	-11.44	-11.44	22 (1)	-7.77	-7.77			
23 (2)	-11.36	-10.87	23 (1)	-7.71	-7.71			
24 (4)	-11.33	-10.02	24 (1)	-7.56	-7.56			
25 (1)	-11.29	-11.29	25 (1)	-7.55	-7.55			

[a] Number in cluster is given in parentheses.

Table 2. The dihedral angles of the conformations of UDP-Gal*p* **1** docked in the active site of UGM.
The dihedral angles are defined as follows: ϕ1 = C2-N1-C1'-O4', ϕ2 = O4'-C4'-C5'-O6', ϕ3 = C4'-C5'-O6'-Pα, ϕ4 = C5'-O6'-Pα-O, ϕ5 = O6'-Pα-O-Pβ, ϕ6 = Pα-O-Pβ-O1'', ϕ7 = O-Pβ-O1''-C1'' and ϕ8 = Pβ-O1''-C1''-O5''.

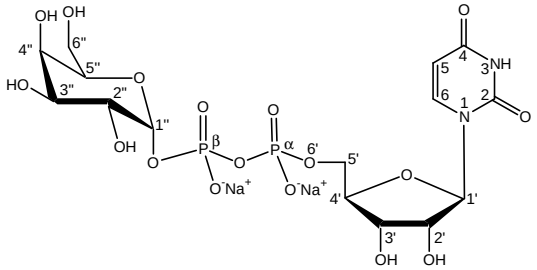

Cluster rank	ϕ1	ϕ2	ϕ3	ϕ4	ϕ5	ϕ6	ϕ7	ϕ8
1	-109.1	148.6	92.8	-126.1	-0.7	-110.9	91.0	-164.7
2	-170.7	-38.3	-91.7	-2.7	149.0	-146.7	162.5	130.4
3	-38.7	92.6	-81.3	138.5	-57.9	-123.2	-138.2	-175.8
4	-52.0	-57.6	103.5	-173.4	-33.8	-119.0	97.9	-172.0
5	-136.3	114.8	-42.8	-153.1	-116.7	-99.8	76.0	139.8
6	-49.2	-3.5	-127.3	-83.4	-120.2	-145.4	29.2	-170.2
7	-127.0	149.6	90.4	-86.4	164.7	-38.4	135.4	111.2
8	-127.6	140.9	118.6	-144.8	-3.8	-75.3	-125.6	170.6
9	74.2	3.2	150.1	-90.0	166.8	-12.4	169.0	149.7
10	60.8	167.9	107.3	-47.5	167.3	68.1	22.8	128.4
11	-158.8	-29.9	-161.9	-95.1	-13.2	161.4	94.5	58.7
12	-87.3	-6.1	62.8	1.0	-152.1	-131.0	74.5	-152.4
13	-105.7	-7.3	149.7	-87.2	27.5	50.5	80.7	143.7
14	68.7	-178.9	120.1	95.6	154.0	57.8	45.8	53.2
15	63.7	128.4	-113.8	-73.9	-77.8	35.5	12.5	120.1
16	72.8	-176.7	123.3	115.2	-38.6	-115.3	-78.1	150.9
17	-66.9	74.4	170.8	-94.0	-103.2	-124.6	-169.6	59.2
18	61.7	79.6	130.1	45.3	-110.2	-140.9	19.4	173.1
19	49.2	-150.5	-83.9	58.9	-123.7	124.8	12.7	82.7
20	171.0	-95.0	120.1	-169.6	55.1	176.5	-165.0	175.2
21	-99.1	-34.7	-139.4	-139.2	-166.8	-3.4	160.4	48.0
22	-34.3	-28.9	103.1	-164.5	-75.8	40.3	108.8	51.5
23	-173.6	173.4	-106.4	134.2	99.7	-32.6	-3.0	106.3
24	-80.9	-45.0	154.7	-58.9	-49.6	-177.2	59.4	132.2
25	-118.2	37.3	107.9	17.5	-165.2	173.0	100.4	66.1

Table 3. Interactions of polar groups of the bound model of UDP-Gal*p* **1** with residues in the active site of UGM.

Groups of **1**	Residues in UGM active site	Distance (Å)
$O\text{-}_{6''}$	Arg A278: NH1	3.15
6''-OH	Arg A278: NH1	2.95
4''-OH	Asn A80: OD1	3.21
4''-OH	FAD: O4	2.85
2''-OH	Tyr A346: OH	2.49
2''-OH	FAD: N5	3.13
1''-OH	Arg A278: NH1	2.78
1''-OH	Arg A278: NH2	2.88
O^{α}	Arg A278: NH1	3.39
O^{α}	Arg A278: NH2	2.51
O^{α}	Tyr A311: OH	3.27
O^{α}	Tyr A311: OH	2.93
O^{β}	Arg A278: NH2	3.13
$O_{-6'}$	Tyr A346: OH	3.47
3'-OH	Gln A155:OE1	3.20
2'-OH	Gln A155:OE1	3.11
2'-OH	Trp A156:NE1	3.38
N1	Ile A167: O	3.19
2-O	Pro A312: O	3.20
N3	Ile A167: O	3.37
N3	Asn A314:OD1	3.00
4-O	Asn A314:OD1	2.59

Figure 1. (A) and (C). Expansions of the reference 1D ^{1}H NMR spectra of UMP morpholidate in the presence of UGM at 600 MHz and 285 K. (B) and (D). the 1D ^{1}H STD-NMR spectra, recorded without water suppression, are shown (U: Uracil; R: Ribose). Proton signals from H1R and H5U are separated well (shown in A and C) and the STD signal from H5U is much weaker than that of H1R. For the STD intensity of the complex of UGM and UDP-Gal*p*, we chose to use the same value for H5U and H6U since similar intensities for H5U and H6U were observed in the UMP-UGM STD spectra.

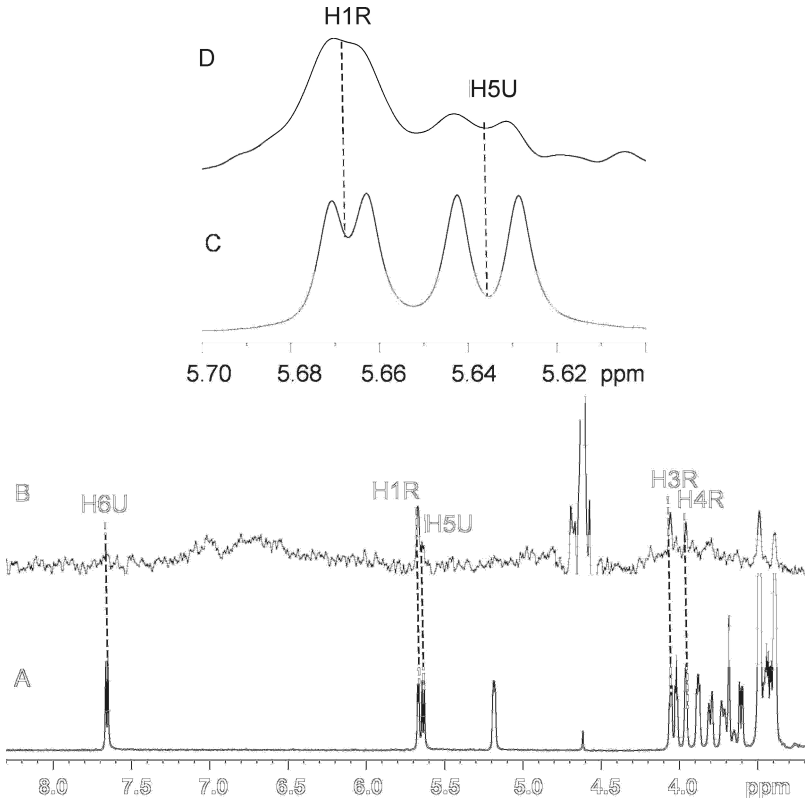

Figure 2. Comparison of experimental and predicted STD values from the CORCEMA-ST protocol for (A) UDP **2** and (B) UDP-Gal*p* **1** in the presence of UGM. (U:Uracil; R:Ribose; G: Galactopyranose). Theoretical STD values (white bar) were predicted by the CORCEMA-ST protocol based on the binding mode of UDP **2** and UDP-Gal*p* **1** generated from the AutoDock for monomer B of UGM. Experimental STD values (grey bar) were calculated as $[((I_{0(k)}- I(t)_{(k)})/I_{0(k)})\times 100]$, with $I_{0(k)}$ being the intensity of the signal of proton k without saturation transfer at time t=0, and $I(t)_k$ being the intensity of proton k after saturation transfer during the saturation time t. The calculations were performed using the following parameters, S^2 = 0.25 for the methyl group, S^2 = 0.85 for methyl–X relaxation; the concentration of ligand was 4mM and the ratio of ligand: protein was 100:1; k_{on} =10^8; K_D = 10 μM; t = 0.3 ns and 50 ns for ligand in free and bound states, respectively. Whether the binding mode of 1 in monomer B was with the structure of the lowest docked energy or the structure similar to that in monomer A, the predicted STD effects for the uridine moiety in UDP-Galp 1 were very weak, in disagreement with the results from STD-NMR experiments. Consequently, higher R-factors (0.6862 and 0.6986 for UDP **2** and UDP-Gal*p* **1,** respectively) were obtained from the calculation by CORCEMA-ST.

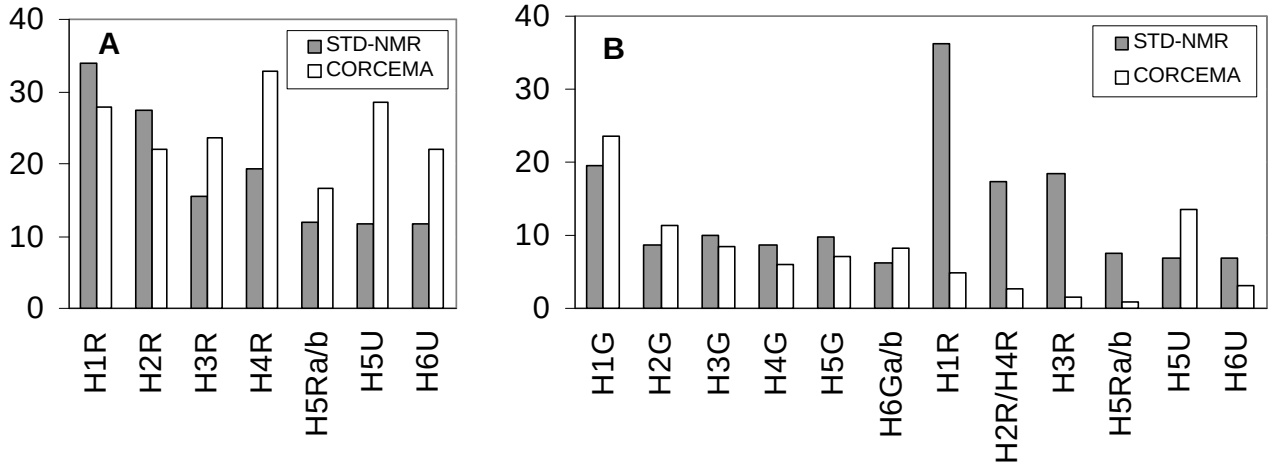

Figure 3. Superposition of monomers A and B of UGM from *E. coli*, and UGM from *K. pneumoniae*, showing the differing positions of the mobile loop and accessibility of the active site. Monomer A is colored red, with the mobile loop colored yellow, monomer B is colored blue with the loop in cyan and UGM from *K. pneumoniae* is colored green with the loop in magenta. The flavin from monomer A is also shown.